Trans. JWRI, Vol. 22 (1993), No.1

Characteristics for Solidification and Transformed Microstructure of Electroslag Weld Metal in Low Carbon Structural Steel †

Fukuhisha MATSUDA*, Yasushi KIKUCHI, Zhong-dong QIAN*** and Shoichiro FUJIHIRA******

Abstract

The characteristics of solidification and transformed microstructures of electroslag(ES) weld metal have been studied in low carbon structural steel. The solidification modes are two classes: one is epitaxial cellular columnar growth in rim zone of weld metal , and other one is axial or stray cellular dendrite columnar growth in core zone. Transformed ferrite is classified by morphology into two types. Type 1 is proeutectoid ferrite which is composed of prior austenite boundary ferrite and intragranular polygonal ferrite. Type 2 is intragranular acicular ferrite. There was no difference in chemical composition between core and rim zone, but the volume fraction of proeutectoid ferrite is extremely different between core and rim zone. The effect of microstructure on impact toughness of ES weld metal is discussed. It is thought that the toughness of ES weld metal was depended on the amount of proeutectoid ferrite and notch direction.

KEY WORDS: (Solidification) (Epitaxial) (Axial) (Stray) (Transformation) (Proeutectoid) (Segregation)

1. Introduction

Electroslag(ES) weld process is being used for four side plate box column construction of steel frame building and other field owing to its beneficial effects on economy and efficiency of production. A significant problem is low toughness of weld metal, and that toughness is different between core and rim zone. It was being conventionally thought that this difference of toughness between core and rim zone resulted from the segregation of impurities occurred in core zone. It is well known that the properties of weldments may be improved markedly by controlling solidification process during welding. The systematic studies for welding solidification in ferrite steel had been performed by Savage and others in 1950-1960's. Solidification mode is related to the $G/(R)^{1/2}$ ratio and solution content, which was described by Tiller and Rutter[1]. There are markedly effects of solidification modes on mechanical properties. The primary arm spacing is an important parameter in cellular(dendrite) columnar growth. But a more important parameter is the distance between the nuclei, or the grain size in equiaxed growth[2]. Although numerous investigators have demonstrated the solidification modes for various welding process, the freeze mode of ES weld metal hasn't been advanced more clearly by the welding metallurgist. It is all known that the impact toughness is closely related to transformed microstructure,is particularly related to the morphology of ferrite in low carbon low alloy steel. Impact value is generally high of fine anisotropic acicular ferrite, low of coarse proeutectoid ferrite[3]. This paper describes the characteristics of solidification mode and ferrite morphology of ES weld metal, and discusses the correlations of solidification and transformed microstructure. The characteristics of impact toughness of ES weld metal are also discussed.

2. Experiment Procedure

2.1 Materials

The chemical compositions of materials used in this study is shown in **Table 1**. Base metal was 40mm thickness plate of $50kgf/mm^2$ grade as SM50A. ES welding wire was commercial wire which is $\phi 1.6$ diameter. The chemical composition of materials used and weld metal were analyzed by conventional wet process. The analyses of nitrogen and oxygen were by courtesy of TC-30 NITROGEN/OXYGEN DETERMINATOR(Leco).

† Received on July 28,1993.

* Professor
** Associate Professor
*** Graduate Student
**** Co-operative Researcher, Katayama Stra•Techs. Ltd.

Transactions of JWRI is published by Welding Research Institute, Osaka University, Ibaraki, Osaka 567, Japan

Table 1 Chemical compositions of base metal and wire used (weight percent)

Materials	C	Si	Mn	P	S	Mo	O	N
SM50A	0.18	0.46	1.45	0.02	0.007	--	0.001	0.003
YM55	0.06	0.42	1.26	0.006	0.002	0.2	--	--

Table 2 Welding conditions of electroslag welding

Sample mark	Current (A)	Valtage (V)	Welding speed (cm/min)	Heat input (KJ/cm)	Flux weight (g)	Diaphragm thickness (mm)	Gap (cm)
ES	380	40	9.0	101	13	15	15
EA	380	42	5.5	175	30	20	20
EB	380	45	3.2	320	55	30	25
EC	380	48	2.4	456	70	40	25
ED	380	50	1.5	790	90	60	25
EL	380	51	0.9	1267	100	80	25

2.2 Welding Conditions

An important parameter of ES welding conditions is welding current which markedly effects the melt pool shape. In this experiment,a constant current (380A) was selected. The variation of heat input was realized by the choices of root gap of diaphragm and welding voltage. The parameters of ESW are shown in **Table 2.**

2.3 Experimental Methods

The samples used for microstructure observation were taken from longitudinal sections parallel to welding direction.These samples were polished by 3μm diamond paste and etched. Etchant used for optical microscopy were:(1) supersaturated picral water solution for solidification microstructure, (2) 3% nital etchant for the room temperature microstructure. The microstructures of weld metals were examined by conventional metalgraph, using light optical microscopy. The primary arm spacing of solidification structure was given by measuring the distance between the primary stalks of cellular (dendrite) columnar crystals under magnification 50 times micrographs. The angles between cellular columnar growth direction and welding direction as a function of location of weld metal were also measured under

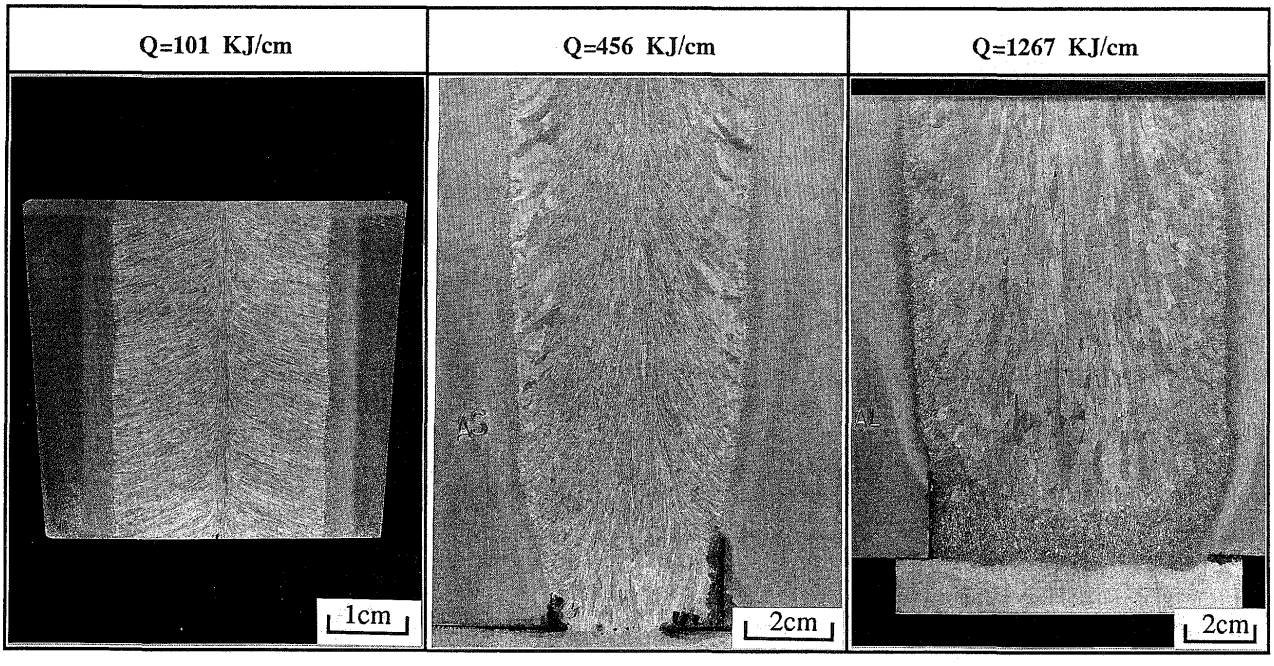

Fig.1 Longitudinal macrostructures of ES weld metal for represented heat input.

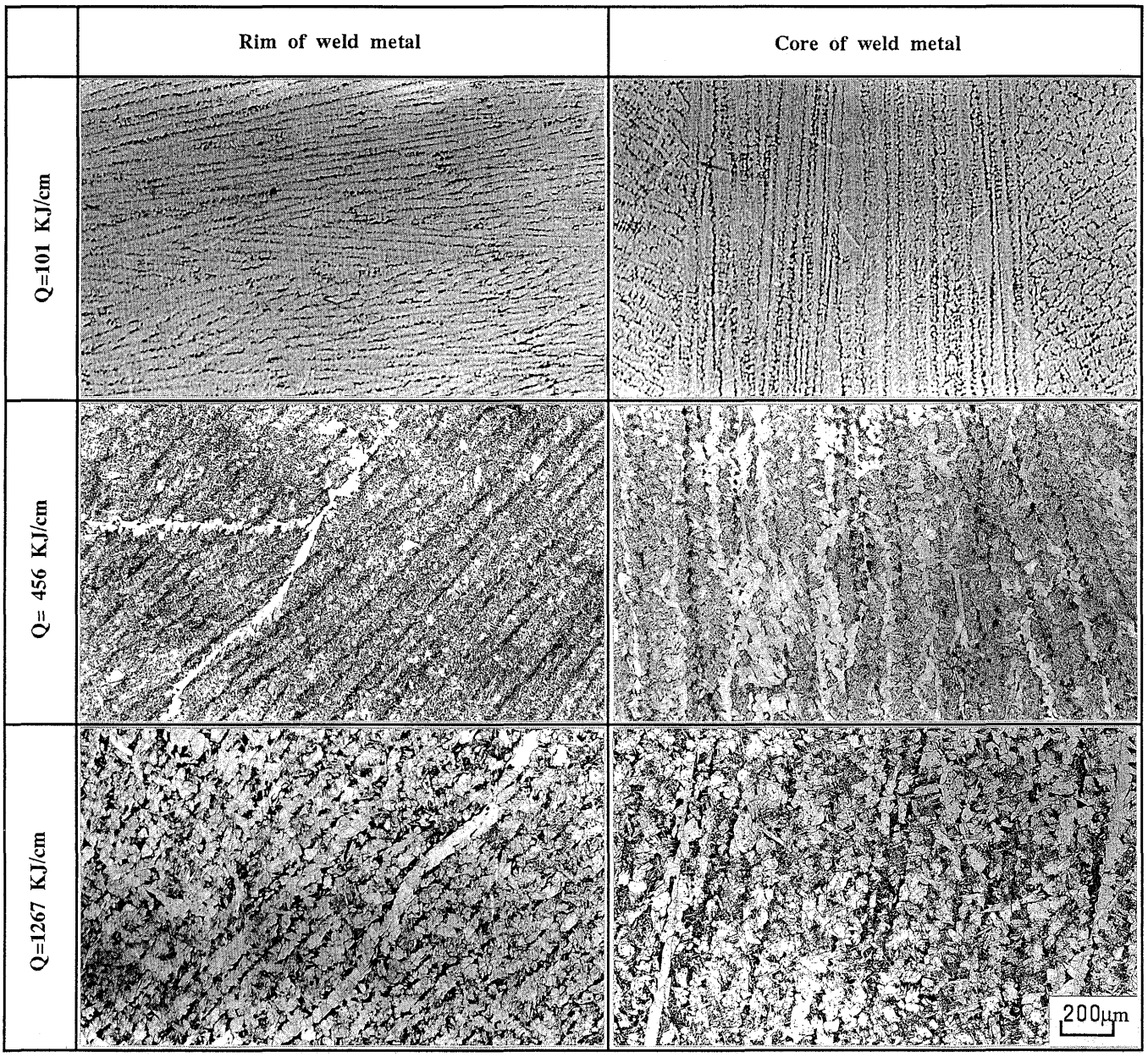

Fig.2 Typical solidification microstructures of weld metal for three heat inputs.

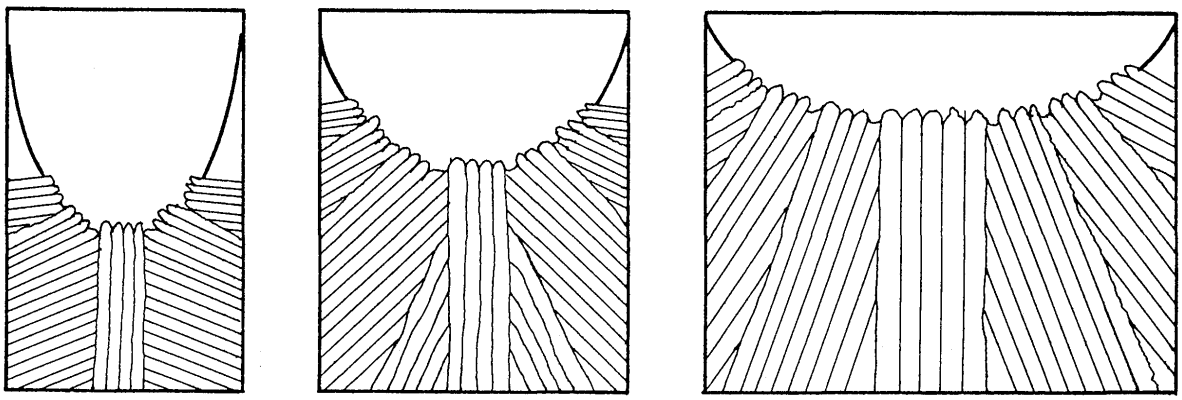

(a) Q=101 KJ/cm (b) Q=456 KJ/cm (c) Q=1267 KJ/cm

Fig.3 Schematic illustrations of solidification microstructures for longitudinal section

magnification 50 times micrographs. The measurements for the volume fraction of proeutectoid ferrite were carried out by means of point counter analysis(at 600 points) under magnification 100 times micrographs.The volume fraction of ferrite was measured by means of image analysis system(LA-525) under magnification 1000 times SEM micrographs. The size of acicular ferrite and grain boundary ferrite was similarly measured under magnification 500 times micrographs. EPMA was used to study the microsegregation at prior austenite grain boundary. The impact toughness was tested at 0°C.

3. Results and Discussion

3.1 Solidification Microstructure

The typical macrographs of ES weld metal are shown in **Fig.1**. It was obvious that on middle heat input weld metal was divided by prior austenite grain size into two zones. In rim zone grains were coarse, but in core zone grains were fine. On low heat input only fine grains were observed, oppositely on high heat input only coarse grains were observed. The solidification micrographs of weld metal with represented heat input are shown in **Fig.2**. The schematic illustration of solidification modes is shown in **Fig.3**.

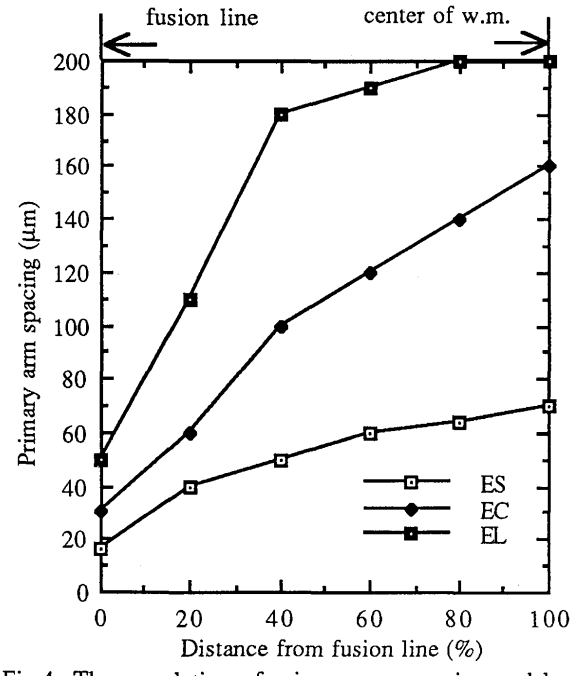

Fig.4 The correlation of primary arm spacing and location in weld metal for three heat input.

The solidification modes are composed of two crystal growths: one is epitaxial cellular columnar growth near to fusion line which grew from unmelt base metal, other one is axial or stary cellular dendrite columnar growth in core zone of weld metal. Equiaxied crystals were not observed in ES weld metal. The modes did not change with heat input, but the primary arm spacing increased with the increase of weld heat input. In same weldments, the cellular columnar crystals grew finely from unmelt base metal in rim zone, and continuously cellular dendnites grew coarsely in core zone. The result of measuring primary arm spacing is shown in **Fig.4**. The orientation of crystal growth is said to be <100> direction and closely aligned with heat extraction direction. **Figure 5** shows the variation of the angle between crystal growth direction and welding direction as a function of location of weld metal for various heat input. The angle varied with location in weld metal. The angle was larger near to fusion line, but was smaller far away fusion line. Near to center of weld metal, the angle suddenly changed and became 0°. The angle was maximum at fusion line (equaled to 90°), was minimum at center line (equaled to 0°).

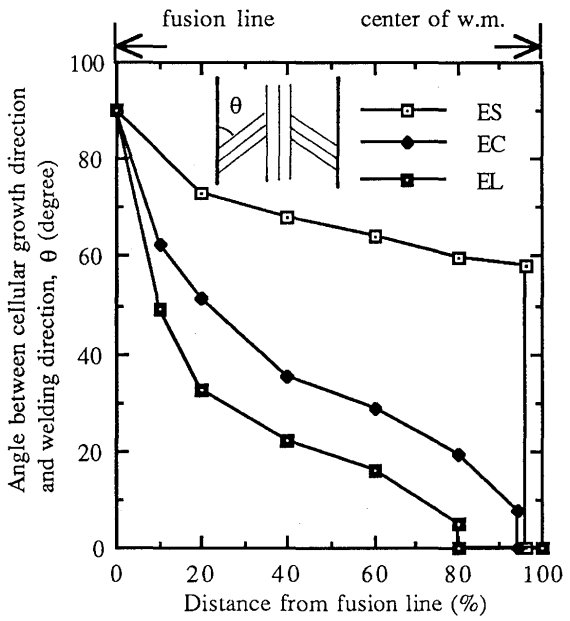

Fig.5 The variation of the angle between crystal growth direction and welding direction as a function of location in weld metal for three weld heat input.

3.2 Possible Mechanism of Fine Zone Formation

The mechanism for the formation of rim and core zone in weld metal were also interested by weld metallurgist. So it is necessary to investigate whether there was a difference in solidification microstructure between core and rim zone. **Figure 6** shows the solidification microstructure and prior austenite grains morphology of the boundary part between core and rim zone. The black dotted lines were solidification cellular boundary, but the white lines were grain boundary ferrite transformed along prior austenite grain boundary. It was clear that cellular columnar crystals grew continuously through prior austenite grain boundary and the interface of core and rim zone. Therefore, the formation of fine austenite grains in core zone was not directly related to solidification microstructure. It is well known that solidification rate is slow in rim zone of ingot

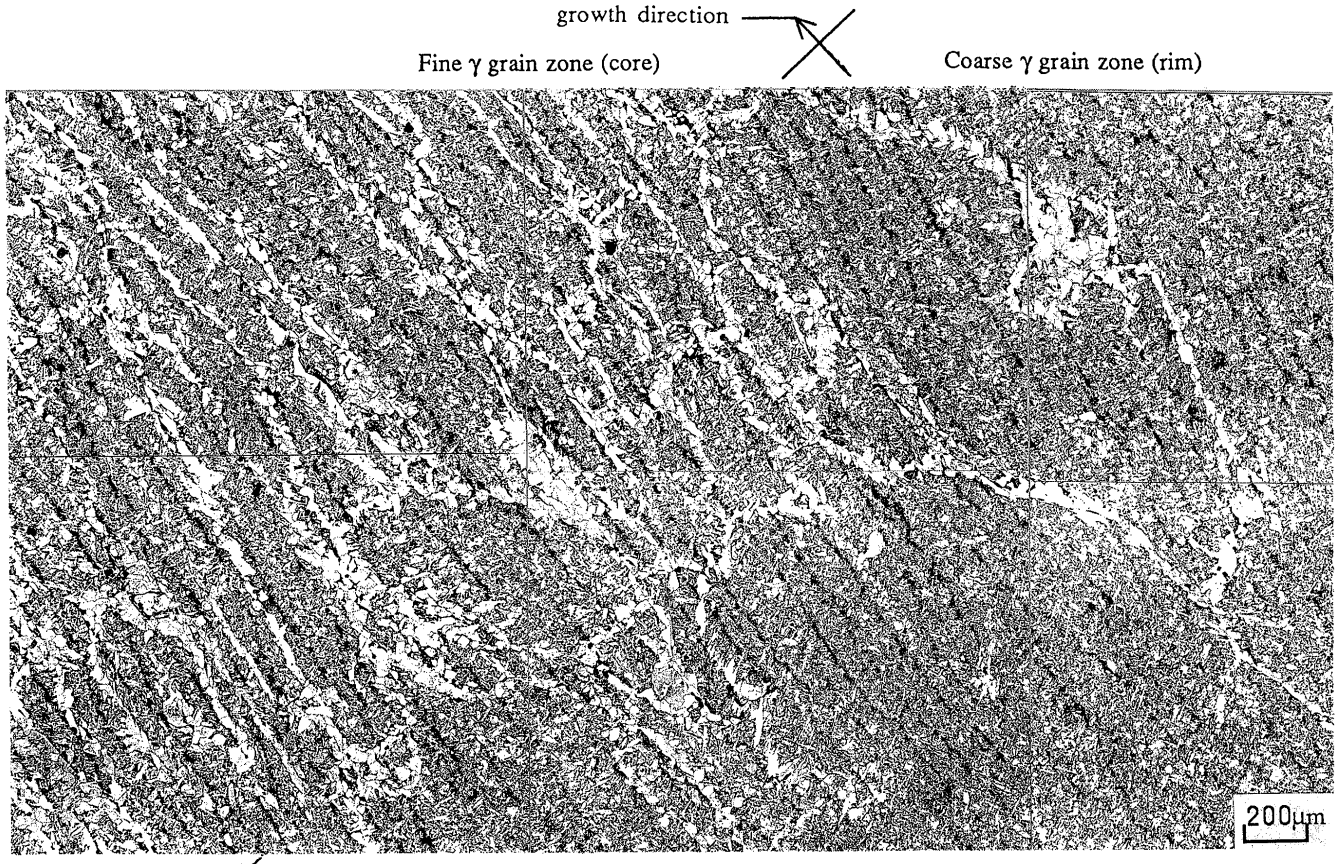

Fig.6 Typical microstrutural change from coarse to fine prior γ grain in 456 KJ/cm weld metal.

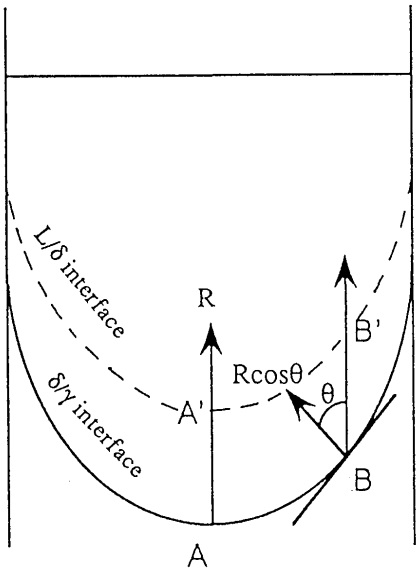

Fig.7 Schematic illustration of solidification and δ/γ transformation front.

in continuous casting, is fast in core zone [4]. Similarly the solidification rate of ES weld metal is slow in rim zone, but is fast in core zone. **Figure 7** shows the schematic illustration of solidification and δ/γ transformation rate (Rcosθ) as a function of location in ES weld metal. The solidification rate equals to welding speed (R) at center of weld metal, but equals to Rcosθ in any location in weld metal. Following is two possible mechanism of fine zone formation that may be thought. First is due to solutes segregation during solidification. These solutes promote austenite grain refinement during δ/γ transformation. It is all known that solutes segregate at boundary of the cellular columnar crystals during solidification. It is assumable that the interaction between solutes and δ/γ grain boundary reduces the grain boundary surface energy, thereby suppressing the grain boundary nucleation. It is also well known that segregated extent is depend on solidification rate. Faster is the solidification rate, larger is the segregated extent. Therefore it may be suggested that rapid δ/γ transformation rate and solutes segregation during solidification are responsible for the fine austenite grains formed in core zone. While the austenite grains grew slowly epitaxially from coarse grains of unmelt base metal in rim zone. Grains were coarse in rim zone.

The second is new nucleation theory. It may be similarly thought that the rate of δ/γ transformation is low in rim zone, but is high in core zone. Transformation rate is the highest at center of weld metal. **Figure 8** shows the schematic illustration of solute distribution near δ/γ interface [5]. Constitutional supercooling is larger for fast growth, but is smaller for slow growth. The austenite grains grew slowly

epitaxially from coarse grains of unmelt base metal in rim zone. No new nuclei formed, so austenite grains were coarse. When grains reached the boundary of core and rim zone, transformation rate was high enough. The constitutional supercooling was large enough to form new nuclei at cellular crystal boundary or coarse inclusions. These nuclei grew rapidly aligning with heat extraction direction. A lot of new nuclei met the requirement of rapid δ/γ transformation. So that fine austenite grain formed in core zone.

By means of micrographs, we can obtain the schematic illustration of prior austenite grain which is shown in **Fig.9**. **Figure 10** shows the size of prior austenite grains as a function of location in weld metal.

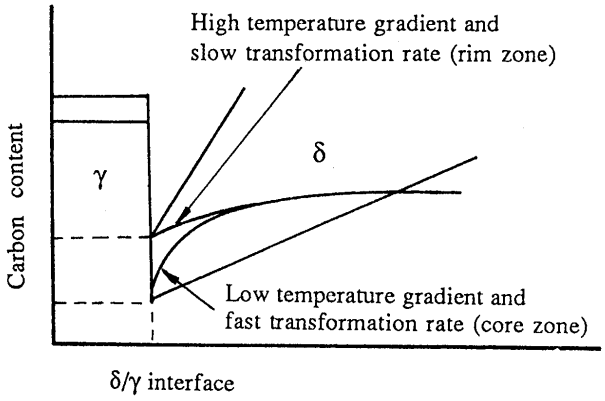

Fig.8 Schematic illustration of solute distribution and temperature gradient near δ/γ interface for rim and core zone in ES weld metal.

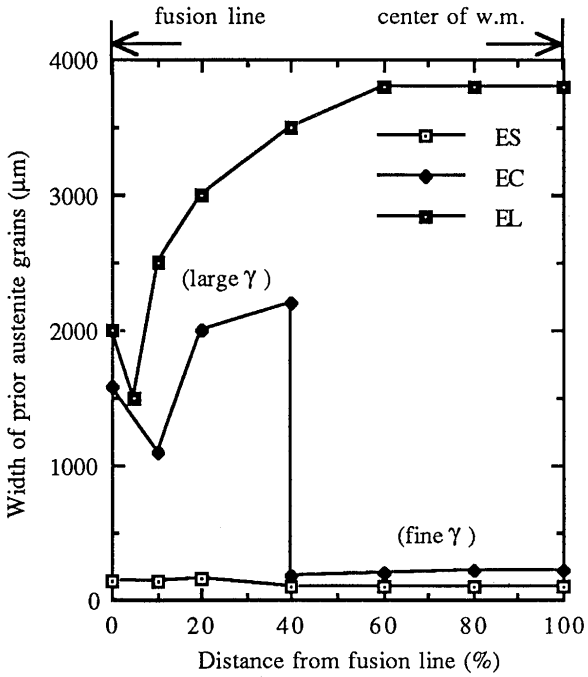

Fig.9 Correlation of prior austenite grains size and location of weld metal for three weld heat inputs.

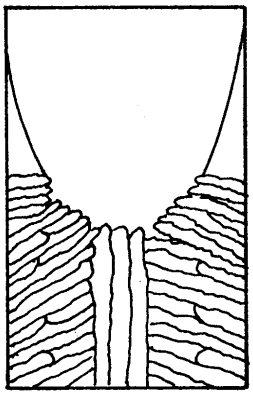

(a) 101 KJ/cm

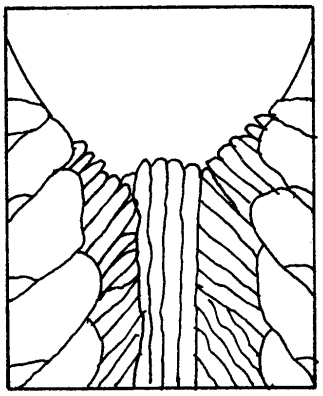

(b) 456 KJ/cm

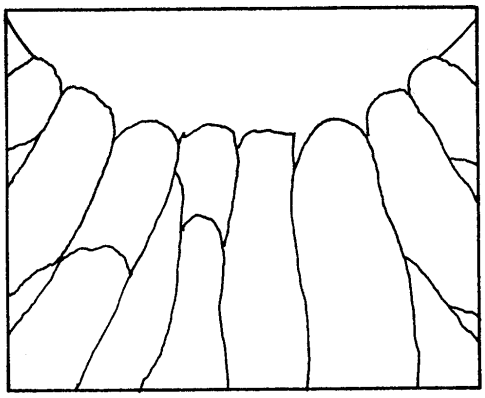

(c) 1267 KJ/cm

Fig.10 Schematic illustration of austenite grain growth. (a) low heat input, (b) middle heat input, (c) high heat input.

For 456 KJ/cm heat input (EC), the growth of rim zone in weld metal stopped at the line which took 40 percent distance between fusion and center line of weld metal. Past this line, core zone formed and austenite grains became finer. The size of prior austenite grains in rim zone was depended on the size of unmelt base metal, but that in core zone was depended on solidification rate and δ/γ transformation rate.

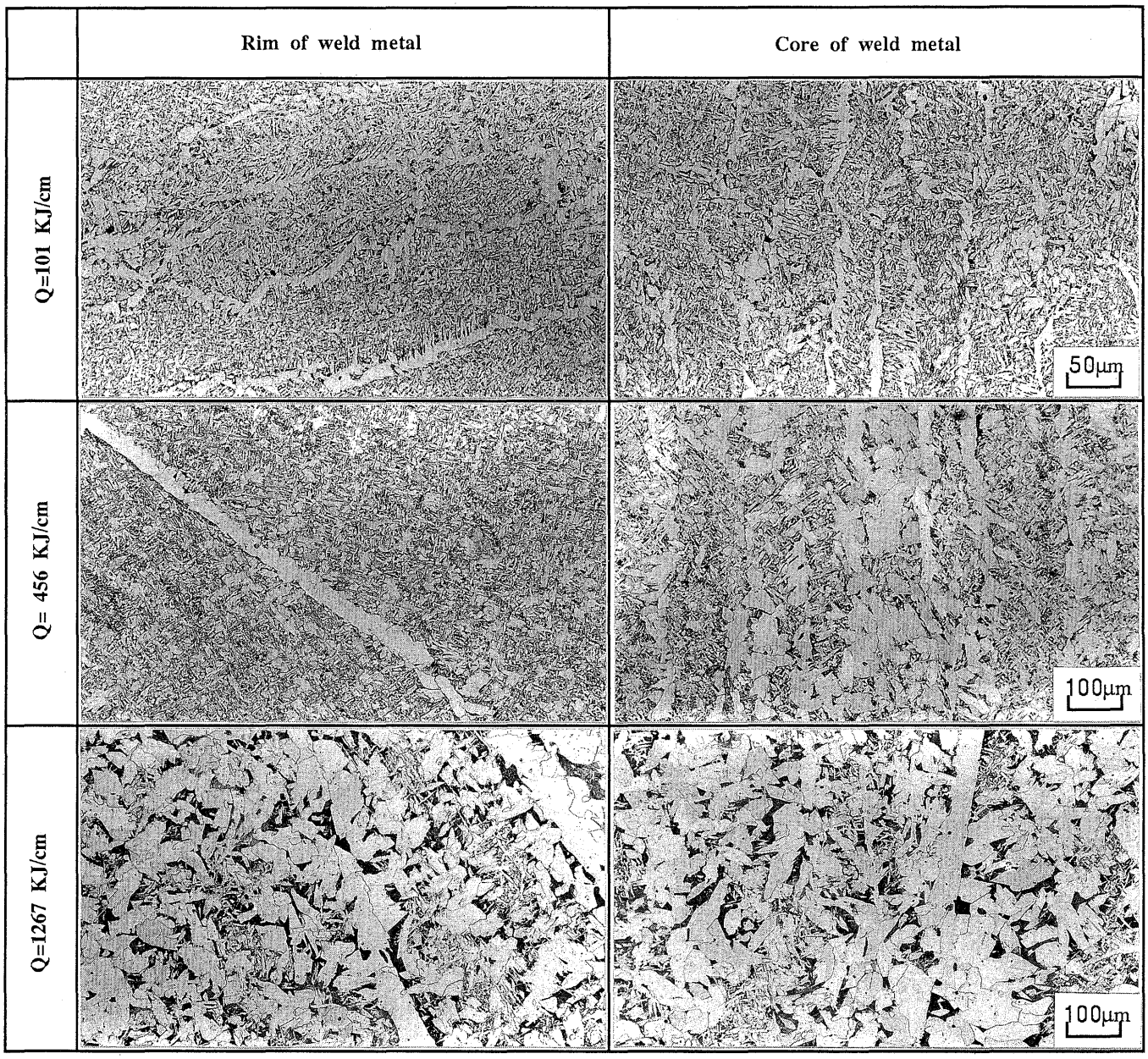

Fig.11 Typical transformed ferrite structure in weld metal.

On the low heat input only fine grains formed owing to small size of austenite grain in HAZ. But on the very high heat input prior austenite grains transformed in very low rate, and no larger constitutional supercooling occurred at δ/γ interface owing to enough time to diffusion of Carbon by low cooling rate. So fine grains did not form in core zone.

3.3 Transformed Microstructure

The properties of weld metal are closely related to transformed microstructure, particularly related to the morphology of ferrite in low carbon low alloy steel. The represented transformed microstructure of ES weld metal is shown in **Fig.11**. The ferrite is classified by morphology into two types. Type 1 is coarse proeutectoid ferrite which is composed of boundary ferrite, side plate ferrite and intragranular polygonal ferrite. Type 2 is fine intragranular acicular ferrite. It has been proposed that proeutectoid ferrite nucleates easily at austenite boundary while acicular ferrite nucleates easily at fine inclusions [6-7].

Figure 12 shows the variation of the amount of proeutectoid ferrite as a function of heat input. **Figure 13** shows the ratios of proeutectoid ferrite and acicular ferrite in core and rim zone of weld metal for 456 and 1267 KJ/cm heat input. The transformation microstructures were composed of ferrite, pearlite and upper bainite. The volume fraction of ferrite took 80

percent of total volume fraction of microstructures. The amount of ferrite in core zone is almost as same as that in rim zone in all weld metals. But the volume fraction of proeutectoid ferrite in core zone of 456 KJ/cm heat input weld metal was markedly more than that in rim zone. The difference in proeutectoid ferrite amount was

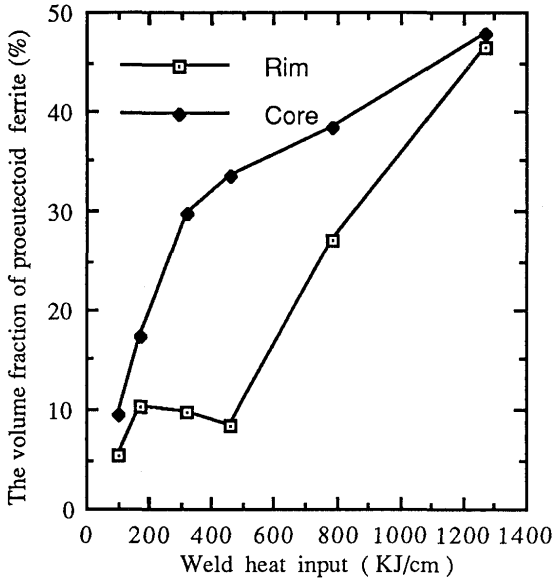

Fig.12 The relationship between volume fraction of proeutectoid ferrite and weld heat input for rim and core zone.

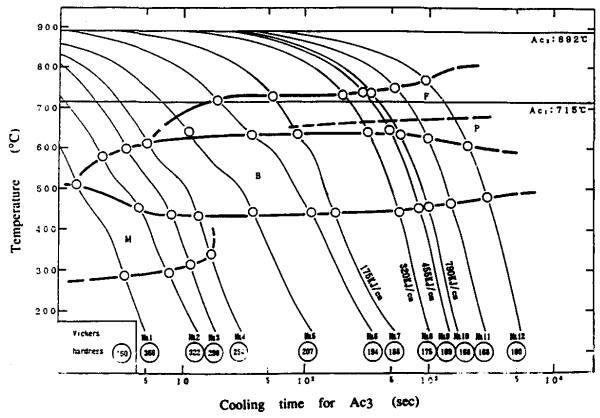

(a) Rim zone.

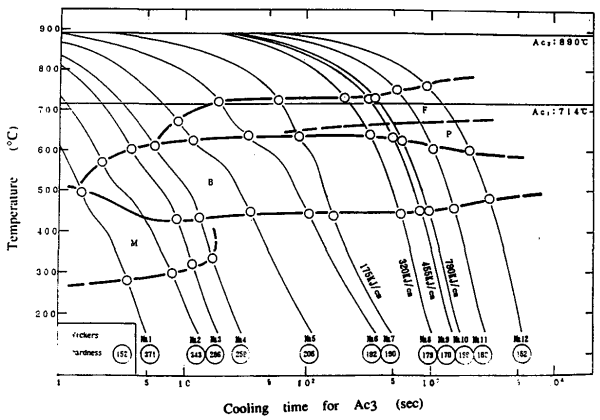

(b) Core zone.

Fig.14 Continuous cooling temperature (CCT) diagram of rim and core zone in 456 KJ/cm heat input weld metal.

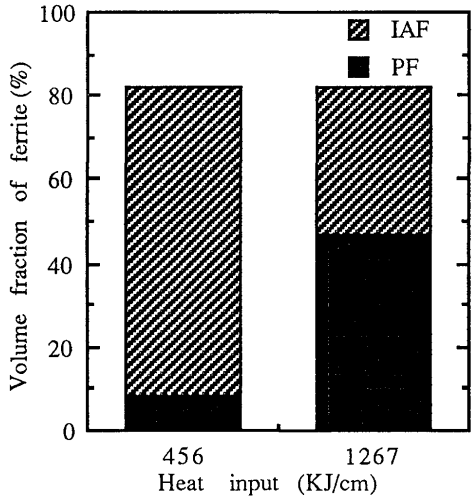

(a) Rim zone

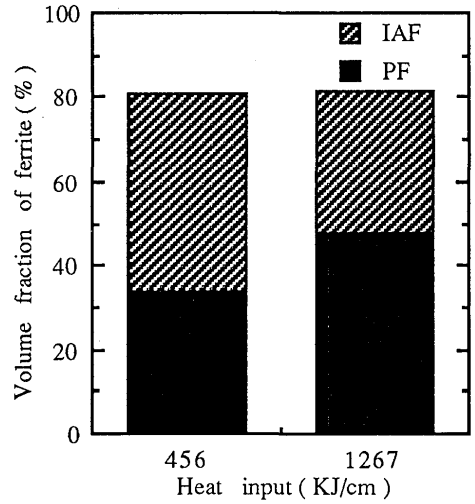

(b) Core zone

Fig.13 The ratio of proeutectoid ferrite and acicular ferrite in weld metal.

the largest in 456 KJ/cm heat input weld metal owing to a lot of grain boundary ferrite formed in core zone, but was less in low heat input or very high heat input weld metal. The amount of proeutectoid ferrite increased with the increase of heat input. Proeutectoid ferrite nucleates and grows easily from prior austenite boundary. Therefore,the large volume fraction of boundary ferrite formed in core zone.

The CCT (continuous cooling temperature) diagram of rim and core zone in 456 KJ/cm weld metal is shown in **Fig.14**. The CCT diagram of core zone was practically as same as that of rim zone.

3.4 Segregation and Inclusions

The properties of weld metal are also varied with the morphology of segregation and inclusions in low carbon steel. During slow cooling proeutectoid ferrite forms also easily at coarse inclusions, so a lot of coarse inclusions would result in coarse ferrite formed. **Table 3** shows the

chemical compositions of core and rim zone. There was no practical difference in compositions between core and rim zone. Macrosegregation had not been observed in ES weldments. EPMA analyses were conducted across prior austenite grain boundaries. In etched specimen, the grain boundary to be analyzed was first marked by using a microhardness tester. The specimen was then polished to remove the etched surface and scanned using EPMA. No specified variation in sulfur, phosphorus and manganese across grain boundary can be seen (**Figure 15**). By means of EPMA analyses, it is clear that the inclusions were mainly composed of Mn-sulfide and Si-Mn-oxide in ES weld metal. **Table 4** shows the content of nitrogen and oxygen in core and rim zone. There was no difference occurred. So it can be thought the morphology and amount of inclusions was same both in core and rim zone.

Table 3 Composition of 456KJ/cm heat input weld metal

Location in weld metal	Composition (%)				
	C	Si	Mn	P	S
Rim of w.m.	0.11	0.40	1.47	0.012	0.004
Core of w. m.	0.11	0.40	1.48	0.011	0.004

Table 4 Content of nitrogen and oxygen in weld metal

Heat input (KJ/cm)	Rim of weld metal		Core of weld metal	
	N(ppm)	O(ppm)	N(ppm)	O(ppm)
101	59	177	58	178
456	44	106	45	107
1267	39	107	38	110

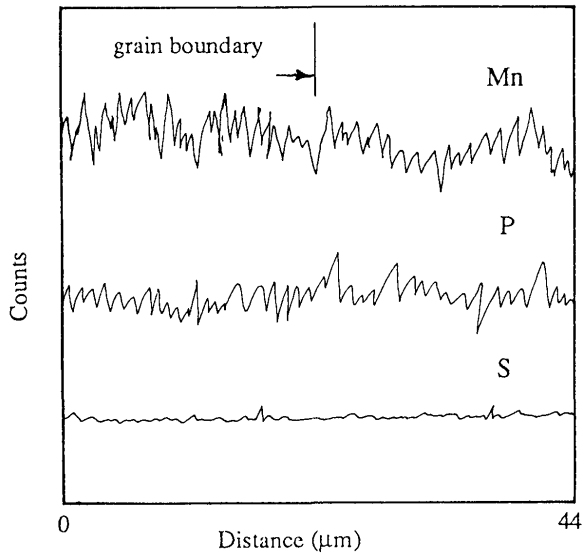

Fig. 15 The variation in sulfur,phosphorus and manganese across prior austenite grain boundary.

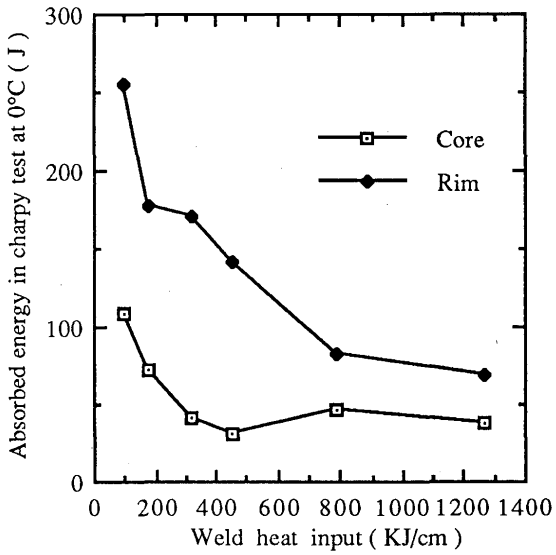

Fig.16 Absorbed energy of weld metal in charpy test.

3.4 Effects of Solidification and Transformed Microstructure on Impact Toughness of Weld Metal

The characteristics of the impact toughness of ES weld metal are shown in **Fig.16.** The impact value of core zone was markedly lower than that of rim zone. This difference of impact value was larger in 456 KJ/cm heat input, but was less on very high heat input. The impact value decreased with the increase of heat input. The effect of notch direction on impact value is shown in **Table 5.** The impact value at center (core) of weld metal decreased in some extent. One reason is due to that cellular columnar growth direction is as same as notch direction. There was no difference in compositions and inclusions in ES weld metal. Therefore it is thought that the decrease of impact value in core zone resulted from the larger amount of proeutectoid ferrite formed and notch direction aligned with cellular columnar growth direction. On very high heat input, the difference in the amount of proeutectoid ferrite between core and rim zone disappeared. So the difference in impact value became less.

Table 5 The effect of notch direction to cellular columnar growth direction on vEa of charpy impact test (456 KJ/cm).

Notch direction	vEa at 0℃ (J)		vEa at -20℃ (J)	
	Rim	Core	Rim	Core
Transverse direction (T)	87.8	35.0	56.0	11.0
Longitudinal direction (L)	74.0	51.9	41.0	15.0

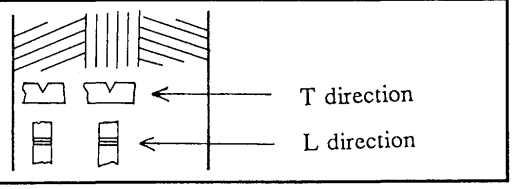

4. Conclusion

(1) The solidification modes of ES weld metal are composed of two crystal growths: one is epitaxial cellular columnar growth which grew from unmelt base metal in rim zone, the other is axial or stary cellular dendrite columnar growth which grew in core zone. The modes had not change with the variation of heat input. Equiaxed growth had not been observed in ES weld metal.

(2) The volume fraction of total ferrite was same both in core and rim zone, but the amount of proeutectoid ferrite in core zone was much more than that in rim zone in middle heat input weld metal. Fine prior austenite grains formed in core zone is responsible for the difference in amount of proeutectoid ferrite between core and rim zone. Generally solidification and δ/γ transformation rate in core zone are more faster than that in rim zone. Therefore,it is thought that more new austenite grains formed finely in core zone during δ/γ transformation owing to fast solidification and rapid δ/γ transformation rate.

(3) There was no difference in chemical compositions between core and rim zone. Microsegregation had not been observed in weld metal using EPMA. There was also no difference in inclusion amount and morphology between core and rim zone.

(4) The impact toughness of ES weld metal was depended on the volume fraction of proeutectoid ferrite and notch direction. Therefore there was a large difference in impact value between core and rim zone in the weld metal for middle weld heat input as 456 KJ/cm.

Acknowledgements

The authors would like to thank Katayama Stra•Techs. Ltd. for valuable support in electroslag welding experiments and charpy tests. Thanks are also to Mr. K. Tomoto for electron probe microanalysis (EPMA).

Reference

1) Tiller,W.A.,and Rutter,J., "The Effect of Growth Conditions Upon the Solidification of a Binary Alloy", Canadian Journal of Physics, 34, P96(1956).

2) W.KURZ, and D.J.FISHER "FUNDAMENTALS OF SOLIDIFICATION", Trans Tech Publications, P85(1984).

3) Yoshinori ITO, and Mutsuo NAKANISHI "Study on Charpy Impact Properties of Weld Metals with Submerged Arc Welding", Sumitomo Kinzoku, July 1975, Vol.27 No.3,P97.

4) Bruce CHALMERS, "PRINCIPLES OF SOLIDIFICATION" Maruzen Co., Ltd. 1971, P226.

5) Ryoseki MISHIMA, "Materials science" NIKKAN KOGYO SHINBUNSHA Co.,Ltd. 1970, P159.

6) D.J.ABSON:Weld World, 1989, Vol.27, P76-101.

7) I.NOMURA, N.IWAMA, and Y.WAKIKADO: Int.Conf.on Physical Metallurgy of Thermechanical Processing of Steels and Other Metals, The Iron and Steel Institute of Japan, Tokyo, 1988, P375-382.